**LIBS Scan Imaging Technology**

Showcasing research from Professor Zhe Wang's laboratory, The Department of Energy and Power Engineering, Tsinghua University, Beijing, China.

Recent advances in chemical composition imaging operation based on laser-induced breakdown spectroscopy

This work provides a comparatively comprehensive and systematic introduction to recent developments in chemical composition imaging based on LIBS, with a focus on principles, operation, and recent developments. More importantly, existing problems in LIBS imaging are illustrated and we provide our own insights into its future development direction, including LIBS signal optimization, LIBS imaging resolution improvement and multiple technology integration.

Image reproduced by permission of Shangyong Zhao and Zhe Wang from *J. Anal. At. Spectrom.*, 2025, 40, 665.

## As featured in:



See Zhe Wang *et al.*,
*J. Anal. At. Spectrom.*, 2025, **40**, 665.

ROYAL SOCIETY OF CHEMISTRY

rsc.li/jaas

## TUTORIAL REVIEW

# Recent advances in chemical composition imaging operation based on laser-induced breakdown spectroscopy

Shangyong Zhao, [a] Yuchen Zhao, [b] Yujia Dai, [a] Ziyuan Liu, [a] Zongyu Hou, [c] Xun Gao [d] and Zhe Wang [*c]

With the rapid development of laser-induced breakdown spectroscopy (LIBS) imaging technology, it has attracted widespread attention. A LIBS imaging system based on laser ablation generates two- and three-dimensional (2D/3D) images through the point scanning method. This paper reviews the recent developments based on LIBS chemical composition imaging technology, including its background, fundamental principles, operation types, applications, and technical upgrade schemes. Here, the types of LIBS imaging operations and proposals for technological upgrades are the focus of this review. More importantly, we point out the existing problems in LIBS imaging and provide our own insights into its future development directions, including LIBS signal optimization, LIBS imaging resolution improvement and multiple technology integration. As a newly recent development direction, the technology fusion method is also a very promising research field in chemical composition imaging based on LIBS. This review is of great significance for the research and application of LIBS chemical composition imaging operations, which will provide basic knowledge guidance for LIBS researchers.

## 1. Introduction

Characterization technology has been playing a big role in research applications such as materials science, biomedicine, industry, agriculture, and environmental science, enabling a better understanding of the morphology, structure, composition, performance, and other characteristics of materials.[1–3] In general, researchers will match the corresponding detection technologies for characterization analysis according to the detection demands for one or more characteristics of the analysis object. For example, the scanning electron microscopy (SEM), laser ablation inductively coupled plasma mass spectrometry (LA-ICP-MS) and other technologies commonly used for comprehensive testing of lithium batteries include experimental techniques such as composition, morphology, crystal structure, functional group, material ion transport observation,

material micromechanical properties, and material surface work function,[4–6] but they are time-consuming and costly. Hence, the diversity of material properties, simplification of operations, and cost savings put forward higher requirements for the traditional detection technology and means.

The proposed chemical composition imaging operation method provides a new research idea and technical direction to solve the above problems, which can provide the distribution of chemical composition on the surface of materials.[7] This operation can simultaneously detect the surface morphology, composition, and other characteristics of the analysis object.[8] Common methods of chemical composition analysis include spectral technology, mass spectrometry, energy spectroscopy, and chromatographic and chemical analyses. In particular, spectral analysis technology has shown a strong development momentum in recent years, and is constantly evolving towards miniaturization, high performance, multi-functionality, intelligence, and green environmental protection, showing great application potential. Typical spectral analysis technologies include ultraviolet radiation (UV),[9] optical emission spectroscopy (OES),[10] Raman spectroscopy (RS),[11] infrared and near-infrared spectroscopy (IR/NIR),[12] X-ray fluorescence spectrometry (XRF),[13] laser-induced breakdown spectroscopy (LIBS),[14] *etc.* Among them, LIBS technology is known as the "future superstar for chemical analysis" due to its advantages such as rapid, *in situ*, micro-invasive, simultaneous multi-element detection, simple operation, and safety.[15] Over recent years, with the continuous improvement of LIBS basic theory and the increasingly mature

*a*Zhejiang A & F University, College of Opto-Electro-Mechanical Engineering, Hangzhou, 311300, P. R. China

*b*Nottingham University Business School China, University of Nottingham Ningbo China, Ningbo, 315100, P. R. China

*c*State Key Laboratory of Power System Operation and Control, Tsinghua-Rio Tinto Joint Research Centre for Resources, Energy and Sustainable Development, International Joint Laboratory on Low Carbon Clean Energy Innovation, Institute for Carbon Neutrality, Department of Energy and Power Engineering, Tsinghua University, Beijing 100084, P. R. China. E-mail: zhewang@tsinghua.edu.cn

*d*School of Science, Ministry of Education Key Laboratory for Cross-Scale Micro and Nano Manufacturing, Changchun University of Science and Technology, Jilin, 130022, P. R. China

This journal is © The Royal Society of Chemistry 2025

*J. Anal. At. Spectrom.*, 2025, 40, 665–678 | **665**

application, chemical composition imaging based on LIBS has become one of the key research highlights.

Compared to other imaging techniques based on chemical element analysis, such as XRF's strict requirements for radiation protection, low sensitivity to light elements, and specific needs for sample preparation, as well as the problems faced by LA-ICP-MS, including high instrument complexity, high cost, complex operation, and high dependence on sample preparation, LIBS imaging technology demonstrates higher cost-effectiveness and wide adaptability. Besides, in contrast to conventional imaging techniques such as SEM, scanning tunneling microscopy (STM), and atomic force microscopy (AFM), LIBS imaging operation starts with point-to-point spectral lines obtained from different locations on the analysis object's surface and goes through the process of elements analysis to create a photograph that contains plenty of information, such as the chemical components and concentration at a certain location, the distribution of edge features, shape features, or texture features of the material surface chemical composition.[16,17] However, this point-to-point approach causes a contradiction between spatial resolution and time consumption. The more point data collected per unit area, the better the spatial resolution, but the collection time will also increase.[18] Furthermore, the instability of LIBS spectra, quantification issues, and the processing of large amounts of data also need to be solved.

Previous work has summarized the principles and applications of LIBS imaging technology.[19,20] This paper aims to provide a comparatively comprehensive and systematic introduction to recent developments in chemical composition imaging based on LIBS, with a focus on the principle, operation, and development of LIBS imaging. We first briefly introduced LIBS technology, LIBS imaging operation, and spectral data processing. Then, the types and applications of LIBS imaging operations were summarized and discussed. Finally, we have put forward some constructive conclusions and suggestions regarding the current situation and existing problems of LIBS imaging operation.

# 2. Fundamental principle

## 2.1 LIBS technology

The schematic diagram of LIBS technology is shown in Fig. 1. A typical LIBS system is composed of a pulse laser, an optical spectrometer, a focusing lens, samples, a two- or three-dimensional (2D/3D) automatic objective table, a coupling lens, optical fibers, and other optical devices.[11,21] When a high-energy pulse laser radiation focuses and is irradiated onto the target surface, after a series of physical processes such as melting, evaporation, expression, cooling, and disappearing, the laser plasma is generated and spectral radiation occurs.[22] Qualitative and quantitative analysis of the elements corresponding to the spectrum is then performed to measure the types and contents of elements in the substance,[23,24] as shown in Fig. 1(a). LIBS technology can detect all elements in the periodic table, and in practical applications, light elements to radioactive elements have been reported,[17] as shown in Fig. 1(b).

## 2.2 LIBS imaging operation

The crater of laser ablation is considered the point or pixel of LIBS imaging, and there are two parameters, the ablative crater diameter and ablative crater depth, as shown in Fig. 2(a). The size and shape of the ablative crater are related to the beam polarization state, focusing diameter, laser energy, sample physical parameters, *etc.*[25-29] By systematically collecting point-to-point spectral information on the sample surface, a LIBS imaging cube $(x, y, \lambda)$ with both positional information $(x, y)$ and spectral information $(\lambda)$ can be obtained,[30] as shown in Fig. 2(b). The principle of LIBS imaging operation is based on the clustering-oriented image segmentation approach, and each minimum subset is called a region of interest (ROI). The greater the ROI per unit area, the higher the spatial resolution of the image, as shown in Fig. 2(c and d). However, the higher resolution of LIBS imaging operation is clearly associated with the longer acquisition time of the source data.[31]
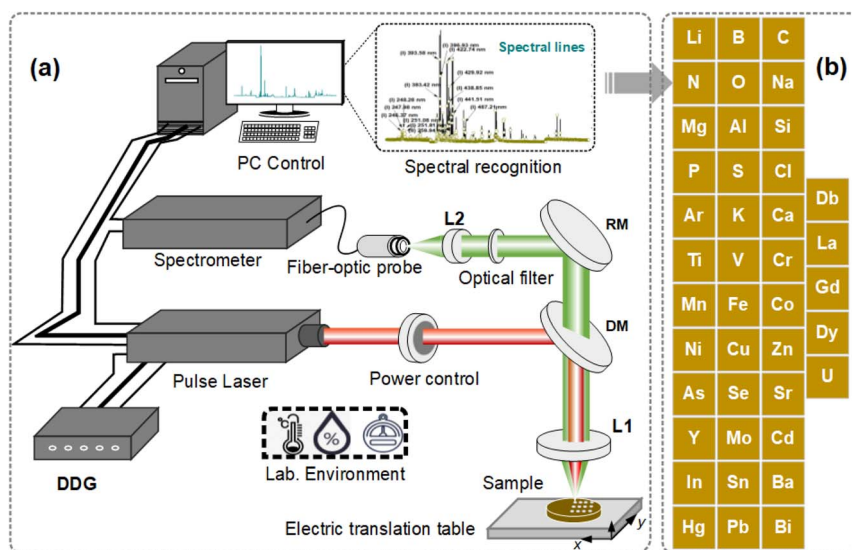


**Fig. 1** Schematic diagram of laser-induced plasma spectroscopy (a) and element detection (b).

**666** | *J. Anal. At. Spectrom.,* 2025, **40**, 665–678

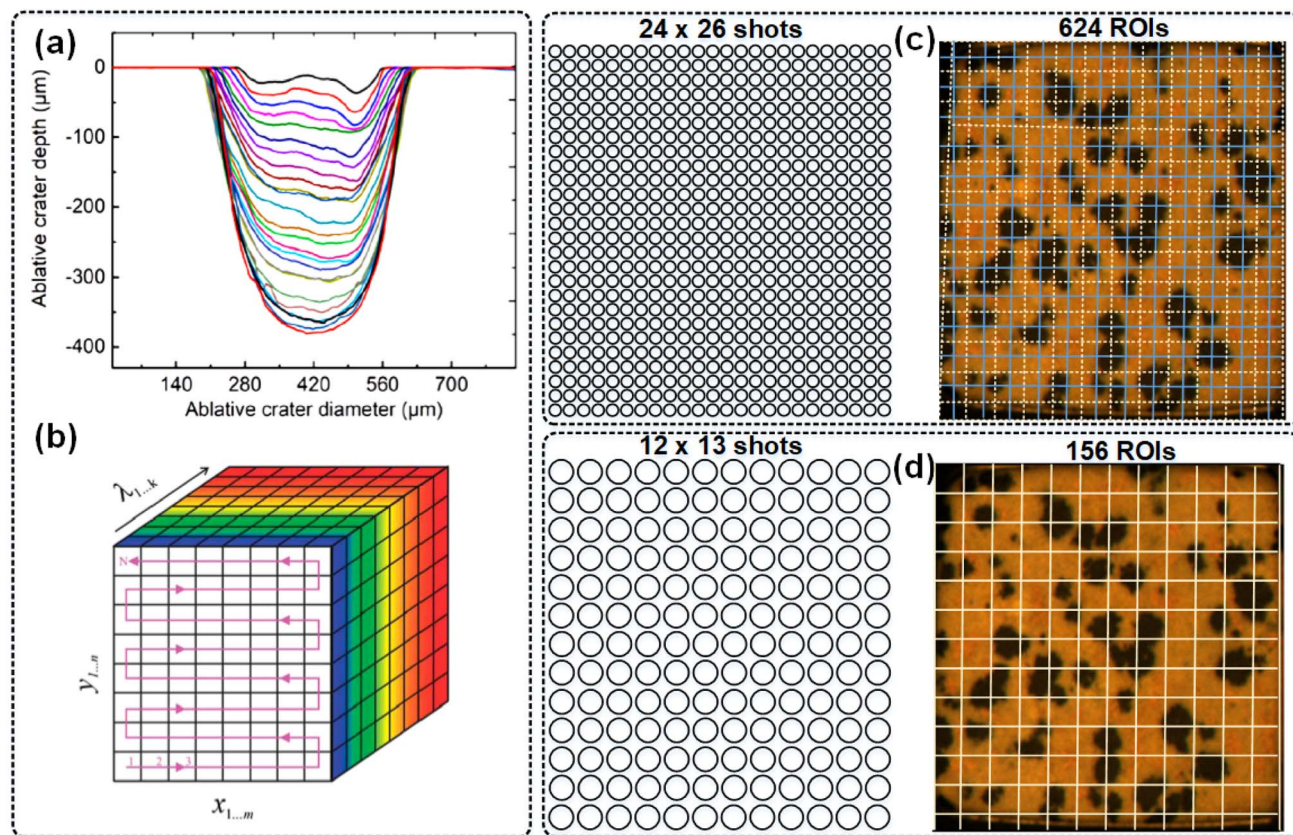This journal is © The Royal Society of Chemistry 2025

Fig. 2    LIBS imaging operation.[25,30,31]

The analytical resolution, spot size, and detection limit of commonly used characterization techniques are shown in Fig. 3. The overall system performance of LIBS is effective, with the minimum size of the detection point reaching several micrometers and the optimal performance detecting the level of hundreds of ppb.[32] In terms of single performance, such as sensitivity and analytical spot size, the advantages of LIBS technology are not obvious, but it is acceptable considering the cost-effectiveness of the technology, including sample processing, instrument complexity and portability, system construction cost, detection ability, and other factors. There is no doubt that LIBS technology still has huge space for further enhancement.[33,34] Besides, compared with traditional imaging analysis techniques like SEM,[35] LIBS also has the capability of chemical composition identification and concentration detection, as well as scanning imaging. As shown in Fig. 3, it can be seen that LIBS technology is in the middle of performance comparison, both of the sensitivity and analytical spot size are better, which means it becomes an attractive alternative to other technologies. In summary, the superiority of chemical composition imaging operations based on LIBS has been well confirmed.

### 2.3    Methodology

The schematic diagram of the original LIBS spectral processing workflow is shown in Fig. 4, which mainly consists of two parts: data preprocessing and LIBS imaging operation. Data preprocessing can significantly improve data quality and make the data more suitable for subsequent analysis and modeling, thereby obtaining more accurate and reliable results.[36] Meanwhile, data preprocessing also helps to improve the execution efficiency of algorithms and the performance of models. And the LIBS imaging operation is to sequentially stitch various ROI segments, which can obtain the distribution of chemical components within the LIBS scanning area, achieving the effect of information visualization.

The spectral preprocessing process and some important modeling tools are as follows: (1) *data dimensionality reduction*: common models include principal component analysis (PCA), linear discriminant analysis (LDA), and *t*-distributed stochastic neighbor embedding (*t*-SNE).[37–39] (2) *Baseline correction*: the baseline correction process can eliminate baseline drift in spectral data and improve data stability and accuracy. Commonly used models include the polynomial fitting method and the least squares method.[40] (3) *Noise removal*: the denoising process can eliminate random noise in spectral data and improve the signal-to-noise ratio, and common models include smooth filtering and wavelet transform.[41] (4) *Standardization*: the standardization process can standardize spectral data to zero mean and unit variance, eliminate the dimensional and magnitude differences in data, and improve its analyzability. Common models include minimum–maximum normalization and standard deviation normalization.[42] (5) *Interpolation*: the interpolation process can be used to
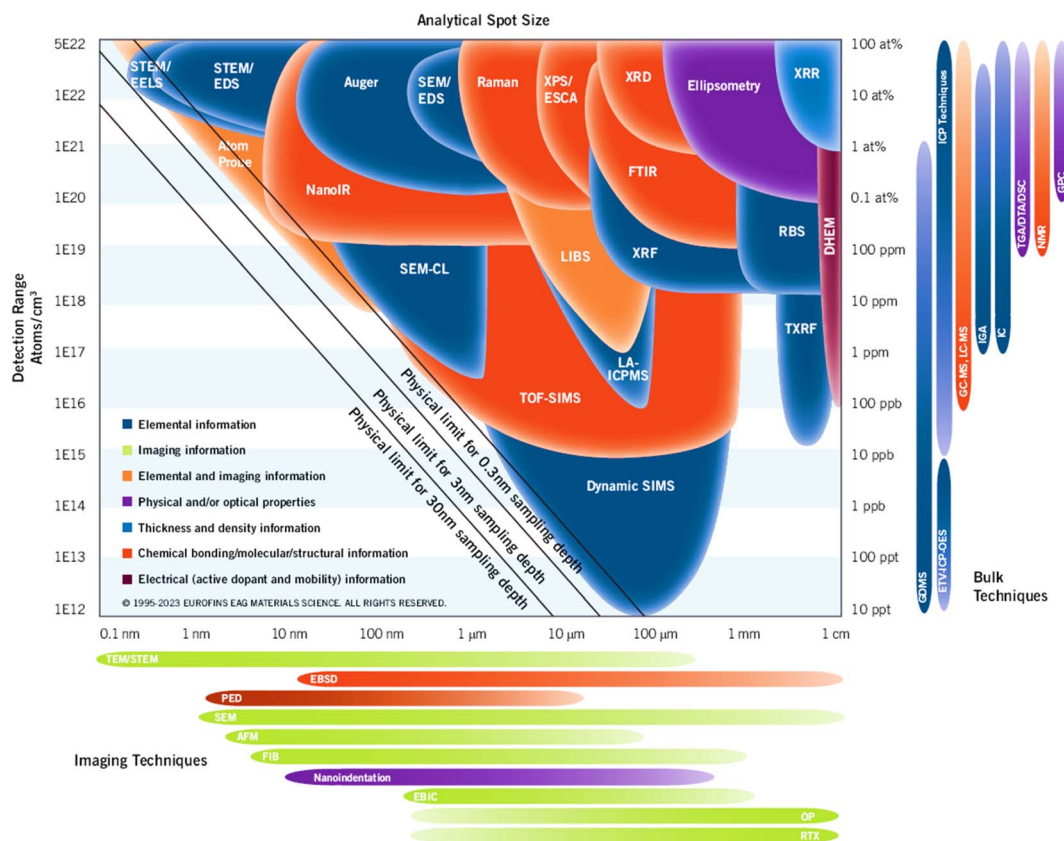
Fig. 3 Analytical resolution, spot size, and detection limit of common characterization techniques (the data source comes from the EAG Laboratories website).

fill missing values in spectral data or smooth out missing values in outlier data to improve data integrity and reliability. Commonly used models include linear interpolation and polynomial interpolation.[43] (6) Principal component selection and identification based on the NIST atomic database.[31] The information obtained through these methods forms the basis for clearly identifying, documenting, and evaluating the importance of each chemical element in matter.
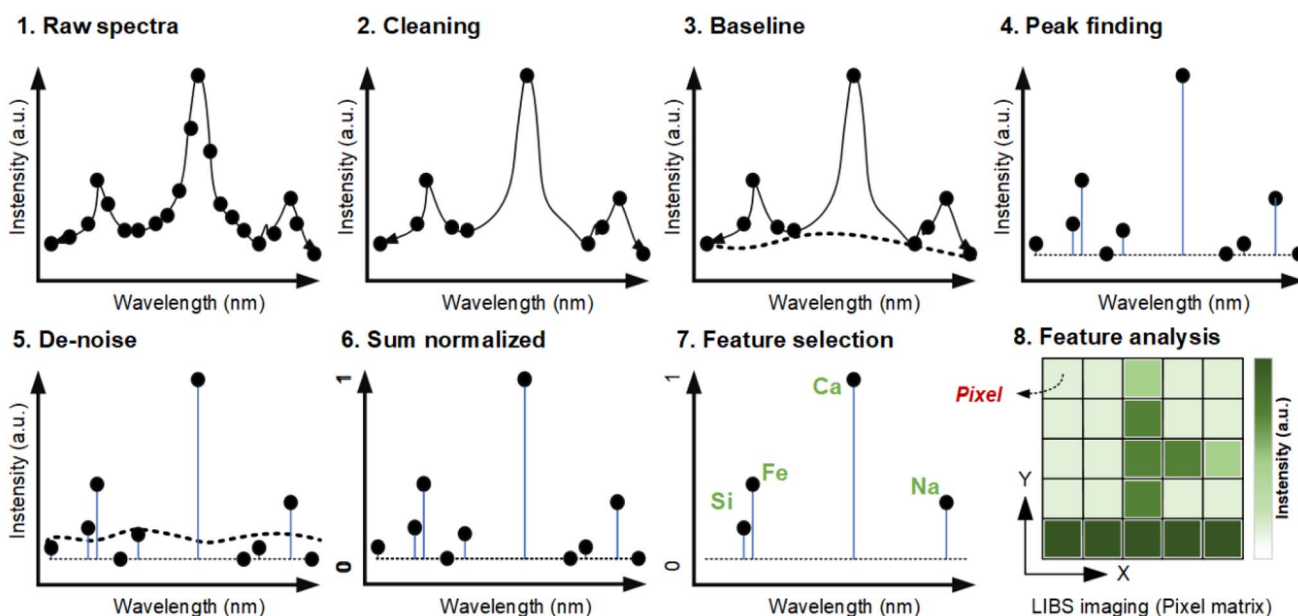


Fig. 4 Schematic diagram of the processing workflow of raw LIBS spectra.

668 | J. Anal. At. Spectrom., 2025, 40, 665–678

This journal is © The Royal Society of Chemistry 2025

The basic principle of LIBS imaging is image region segmentation and stitching, which involves the orderly arrangement of multiple segments (or pixels) of the ROI.[31] Each pixel corresponds to a spectrum, which contains many variables (*i.e.*, spectral lines of different elements in the material after excitation, such as Si, Fe, Ga, and Na, as shown in Fig. 1(b) and 4). In general, most of the reported research work is based on semi-quantitative analysis of characteristic variables, that is, the element distribution and corresponding spectral intensity of LIBS imaging. However, it still remains a challenge to predict the concentration of each pixel in a substance more accurately and precisely. The existing solution is assisted by other technologies, such as ICP-MS, which will be discussed in Section 5. In addition, the number of pixels can reach 2 million over a surface of 488 $mm^2$ with a step resolution reaching 15 μm,[30] and how to deal with such a large scale of data is still the major problem that computer hardware devices and software tools will face.[19,20]

# 3. Types of LIBS imaging operation

## 3.1 Laser device selection

The morphology and formation of surface and internal craters also depend on the laser pulse width, as shown in Fig. 5(a). There are three main pulse-width types of laser sources commonly used in LIBS, including nanosecond (ns), picosecond (ps), and femtosecond (fs) lasers, among which ns lasers are the most widely used.[44–47] The mechanisms that lead to energy absorption and target ablation are entirely different in both cases. During the laser pulse duration, fs-LIBS greatly reduces thermal damage and the heat-affected zone of the target due to negligible heat conduction and hydrodynamic motion. In addition, the spatial resolution obtained by fs pulses is superior to that of ns pulses. Other advantages of fs-LIBS

compared to ns-LIBS include reduced mixing of continuum and atmospheric plasma, as well as the generation of atomic plumes. However, the main disadvantages of fs lasers compared with ns lasers include high equipment cost, high technical requirements, strict environmental requirements, and unknown long-term effects. But with the development of fs laser technology, we believe that its cost performance will continue to improve and its applicability will be increasingly wide. At present, it is regrettable that we have not found the "right way" to use it and can only say that the fs laser has great potential for future development in the field of LIBS imaging.

## 3.2 LIBS 2D/3D imaging

As shown in Fig. 5(b), the LIBS 2D/3D imaging operation is based on the number of pulse shots, with single-pulse shooting and multi-pulse shooting corresponding to two types of 2D imaging and 3D imaging, respectively. In the case of multiple laser pulses striking the same position on the target material surface, the depth of the crater increases with the number of strikes (see Fig. 2(a)),[48] and a 3D LIBS imaging data cube ($x$, $y$, $z$, $\lambda$) with both positional information ($x$, $y$, $z$) and spectral information ($\lambda$) can be obtained (see Fig. 5(b)). Therefore, the 3D imaging of LIBS technology is realized by adding depth information on the basis of 2D imaging. This usually requires changing the focusing position or scanning path of the laser beam to obtain the distribution information of elements at different depths in the sample. Then, these 2D images with different depths are superimposed by computer image processing technology to form a 3D element distribution image of the sample. It can be said that the 2D imaging of LIBS technology can quickly obtain the element distribution information on the sample surface, while the 3D imaging can further reveal the internal structure and element distribution characteristics of the sample.
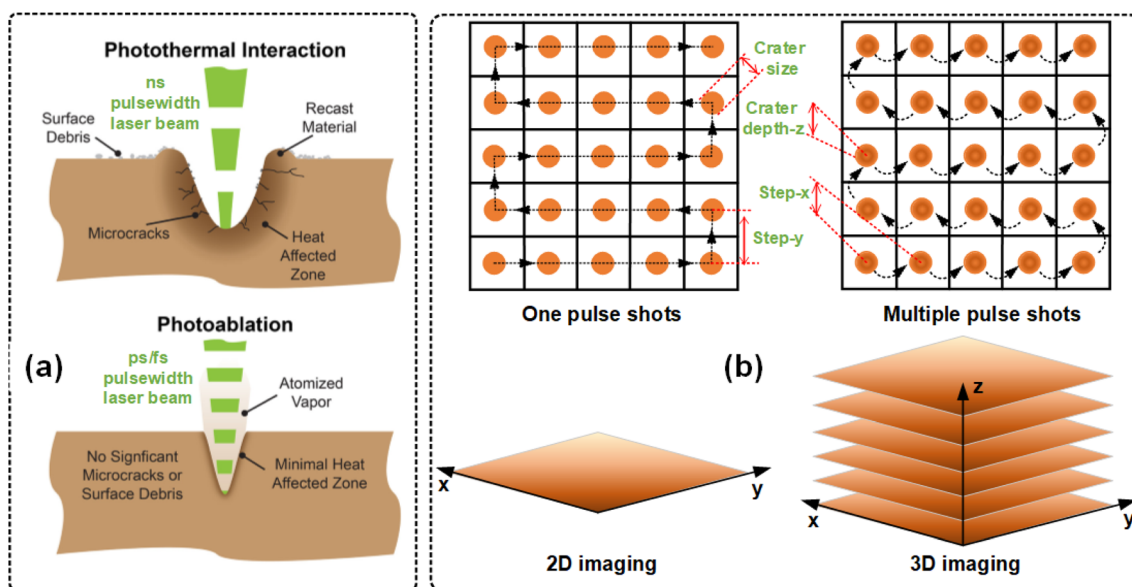


Fig. 5 Schematic diagram of LIBS 2D/3D imaging operation: the (a) method of laser bombardments (the data source comes from the Coherent website) and (b) number of laser bombardments.

### 3.3 Micro-LIBS imaging

Micro-LIBS, or μ-LIBS, is a new element analysis technique based on the combination of LIBS technology and microscopic optics.[49,50] Compared with the traditional LIBS imaging method, the μ-LIBS imaging method has smaller laser energy and focusing spots. The μ-LIBS system employs μJ energy laser pulses for laser ablation, which can achieve minimally invasive craters, high-spectral resolution composition detection, and high-spatial resolution (laser spot size <10 μm). Besides, μ-LIBS can also complete point-to-point scanning detection and analysis of the target object by docking with the precision load displacement platform. The lower μJ laser power allows the sample to be very small in volume (about 10 to $10^3$ μm$^3$) and in mass (10 pg to ng). Meanwhile, μ-LIBS also has good compatibility with Raman technology, and multifunctional detection of elements and molecular groups can be achieved by using the combined LIBS-Raman operation.[51] Compared with the μ-LIBS system, traditional LIBS technology uses laser energy and spot size ranging from dozens to hundreds μm and mm levels, respectively.[52,53] Based on the analysis of target size and dimensions, LIBS and micro-LIBS imaging should consider the actual situation of chemical composition imaging operations.
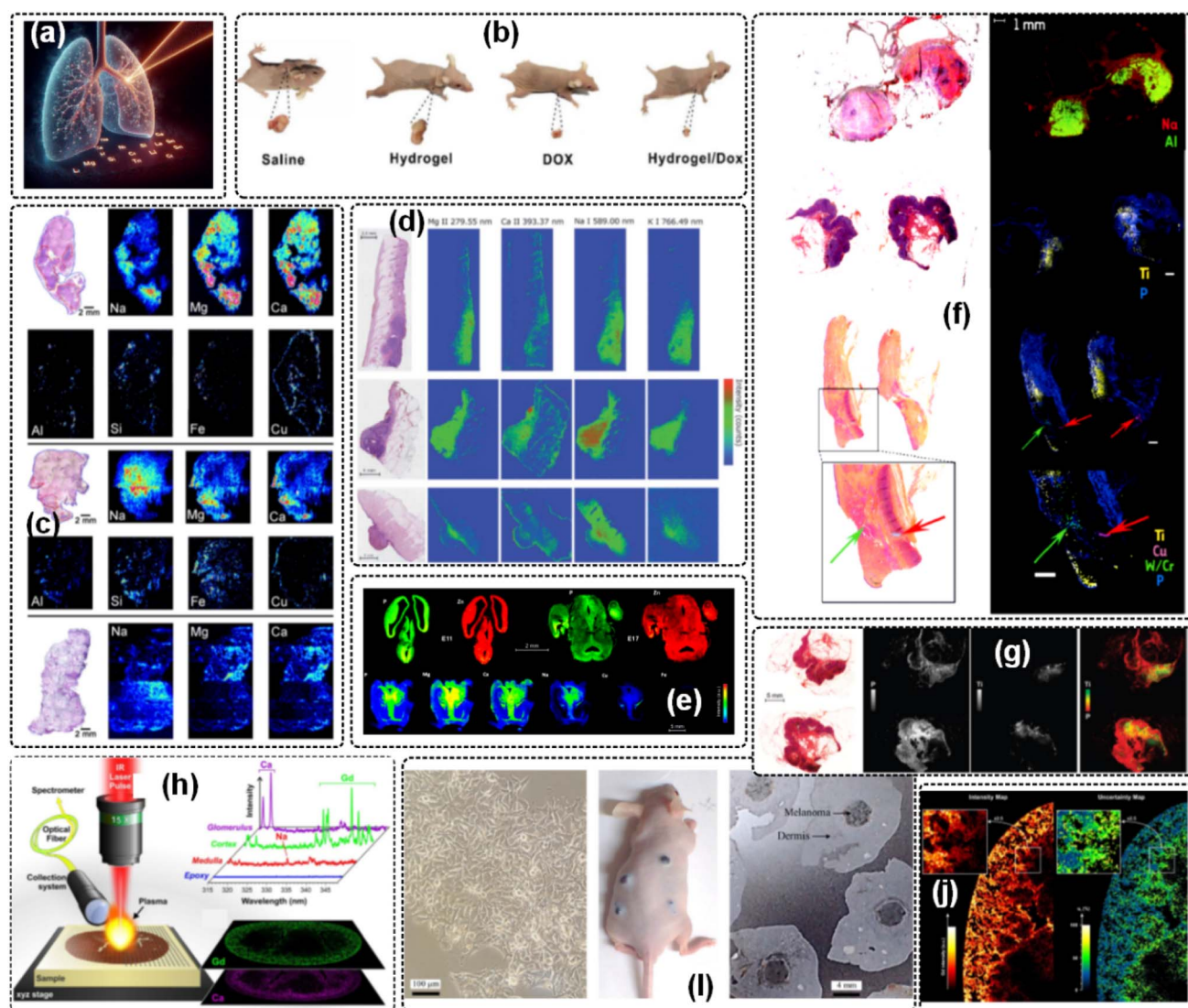


Fig. 6 Biomedicine analysis by the LIBS imaging approach: (a) enhancing diagnostic capabilities for occupational lung diseases using LIBS imaging on biopsy tissue,[59] (b) the representative breast cancer xenograft tumor mice after tail vein injection of 0.9% saline, 100 μg mL$^{-1}$ DOX, hydrogel/DOX (125 μm DNA nanohydrogels, 100 μg mL$^{-1}$ DOX), and 125 μm DNA nanohydrogels, respectively,[61] (c) multi-elemental imaging of different lung tissue types,[63] (d) histological H & E images complemented with LIBS elemental images of Mg, Ca, Na, and K for selected tumor samples,[64] (e) spatio-temporal comparison for P and Zn elements, and an example of various elemental images in a selected section of the brain of a mouse,[66] (f) high-resolution HES histological images a healthy skin sample before LIBS analysis,[65] (g) titanium accumulation in a lymph node,[68] (h) general protocol for LIBS imaging,[67] (i) microscope image of 70% cell confluence, clinical images of mice after 10 days of subcutaneous melanoma cell implantation, and optical image of cryosectioned tissues for LIBS mapping, respectively,[69] and (j) elemental images of Gd distribution in a murine kidney.[70]

670 | J. Anal. At. Spectrom., 2025, 40, 665–678

This journal is © The Royal Society of Chemistry 2025

# 4. LIBS imaging application

## 4.1 Biomedicine

Minor changes in elements within living organisms can directly affect their metabolism and physiological processes. The correlation between the composition and content of elements in organisms and the development of biological metabolism and diseases has been widely studied and has become important supporting information for medical diagnosis and treatment. Studies have found that some essential biological elements participate in oxidation reverse reactions, regulate biological metabolic balance, control biological processes, and have adaptive immune regulation functions.[54–58] In recent years, LIBS imaging has been continuously enhanced as an influential biomedicine technique, showing intriguing potential in the field of clinical and medical analysis, such as for occupational lung disease,[59] tablet coating,[60] human breast cancer,[61] lung tumor,[62] lung cancer,[63] skin tumor,[64,65] cerebral distribution,[66] human tissue,[67,68] clinical specimens,[69] and melanoma tissue.[70] Some of the application results and diagrams are shown in Fig. 6. On the basis of 2D LIBS imaging operations, 3D LIBS imaging is investigated. There are two methods to collect longitudinal data: multiple pulse shots[71] and slice-by-slice cutting,[72] and then a 3D database is constructed. Generally, the former is used for the analysis of solid samples (with a small longitudinal depth and hundred-micron scale), while the latter is used for three-dimensional imaging analysis of biological tissues (with a large longitudinal depth and complex operation).

## 4.2 Minerals

The mineral composition and ore structure are key factors affecting the sustained economic extraction of base and precious metals and require in-depth understanding from upstream ore characterization, metallurgical testing, and process design, to mineral processing. Therefore, mineral analysis is an important basis and premise for geological work and the mining industry, which helps researchers obtain mineral information in time and quickly understand the physical and chemical properties of a certain region or a certain type of mineral.[73] At present, LIBS imaging has been applied to mineral phases,[30,74,75] luminescence phenomena,[76] trace compounds,[77] rock classification,[78] mineral core surfaces,[79] irregularly shaped minerals,[80] elemental identification,[81–83] heterogeneous inorganic archaeological samples,[84] uranium mineralization in uranium ores,[85] and other aspects. Part of the application results and schematic diagrams are shown in Fig. 7. Besides, multiple combined techniques have been applied for mineral analysis, improving the diversity of mineral detection information. Existing methods include LIBS-RS,[86] LIBS-HSI,[87–89] Micro-LIBS/Micro-XRF,[90] and LIBS/LA-ICP-MS.[91] Finally, the research on data processing algorithms (such as principal component analysis, feature lines selection),[92,93] double pulse Micro-LIBS,[94,95] miniaturized devices,[96] etc. Finally, the matching technology and data analysis methods for large-scale and small-scale

scanning objects have further optimized the application of imaging technology in the field of mineral analysis.[97,98]

## 4.3 Industry and materials

Due to the simple sample preparation, fast analysis speed, remote online telemetry, 2D/3D surface distribution, and multi-element depth analysis, LIBS imaging operation has attracted the attention of researchers in the industrial and materials fields.[25,31] LIBS imaging has the characteristics of real-time monitoring of the production process, traceability of detection data, representative analysis data, industrial transmission of data, product quality alarm function, simultaneous detection of multi-component parameters, etc., so it has great advantages in the quality control of industrial production processes. In recent years, the application results and diagrams of LIBS imaging in metal scrap identification,[99] fluoropolymer materials,[100] building materials,[101] Li-ion solid-state electrolytes,[102] trace metal impurity diffusion,[103] fresh impregnated catalysts,[104] mineral fertilizers,[105] printed circuit board compositions,[106] lithium phosphorus oxide thin films,[107] superconductor thin films,[108] and others,[109–111] and the typical work (ref. 97, 102, 104, 106 and 107) are shown in Fig. 8. In addition, three-dimensional elemental imaging of material surfaces[112] and nanoscale subcellular resolution imaging[113] based on LIBS technology have also been studied. Moreover, related research work on quantitative LIBS imaging based on the multiple-calibration approach[114] and LIBS-ICP-MS[115] has been carried out.

## 4.4 Other applications

In order to investigate changes in ancient climate, such as precipitation, major climate changes on Earth, and changes in biological growth processes, there have been reports of extracting reference ancient climate data from fossil samples based on element distribution imaging technology.[116,117] Also, LIBS imaging technology can monitor the environment and growth status of seeds and plant samples, including detecting the absorption, transportation, and accumulation of relevant elements (including nutrients and toxic elements), which is of great significance for understanding the growth status of plant samples, environmental quality, and the interaction between plants and the environment.[118–121] Besides, LIBS imaging technology has shown great application potential in food safety,[122] public security investigation,[123] archaeological mortar,[124] extraterrestrial exploration,[125] and other fields.

# 5. LIBS imaging development

## 5.1 Basic requirements in LIBS imaging

Currently, LIBS imaging technology is still in the stage of qualitative analysis, and how to achieve quantification is a problem that needs to be solved in the future.[126,127] The traditional LIBS quantitative method is based on standard samples. Because the signal intensity of atomic spectral lines can reflect the quantitative relationship corresponding to element content, for samples with high purity and a simple structure, the quantitative method based on standard samples
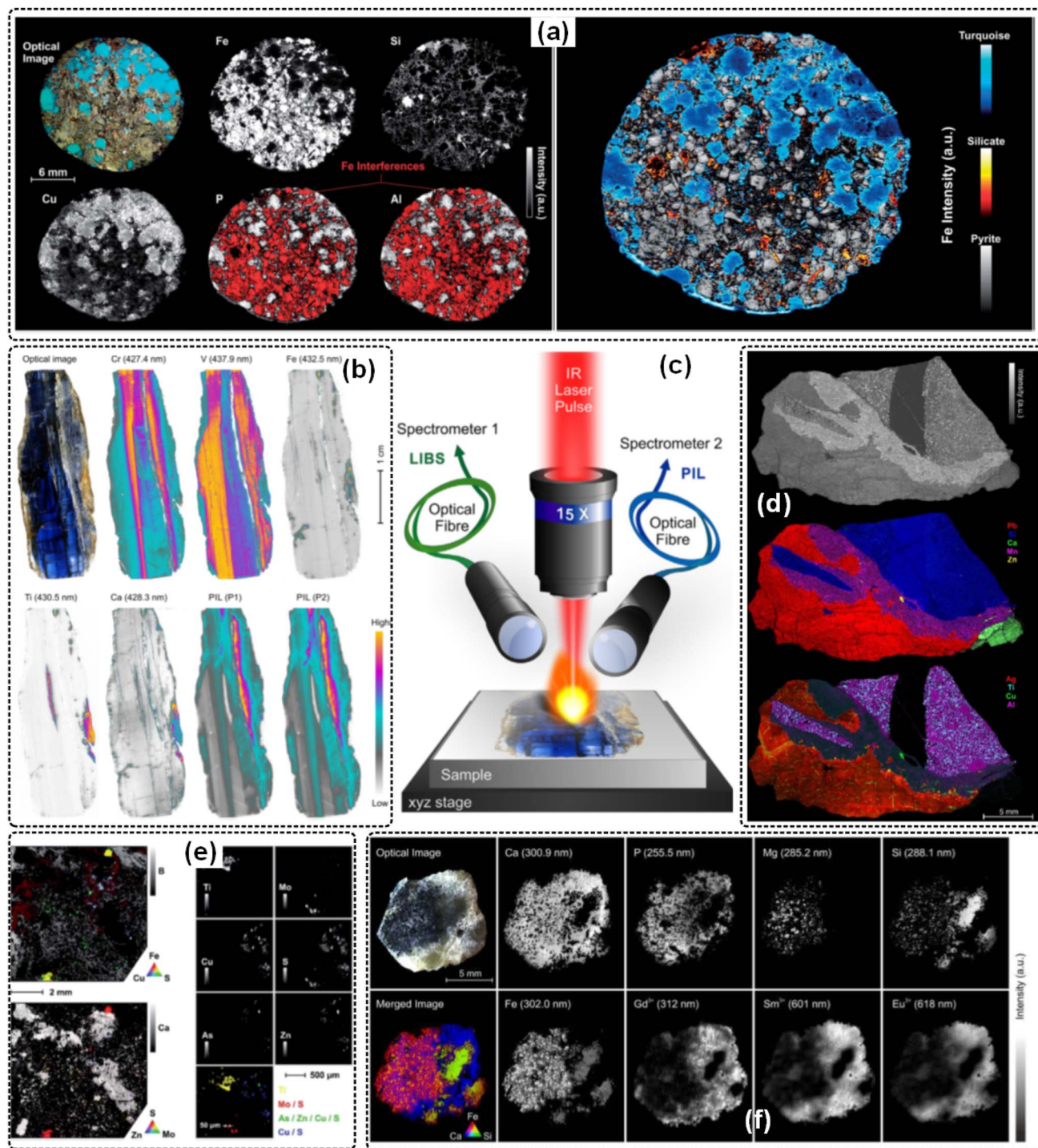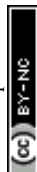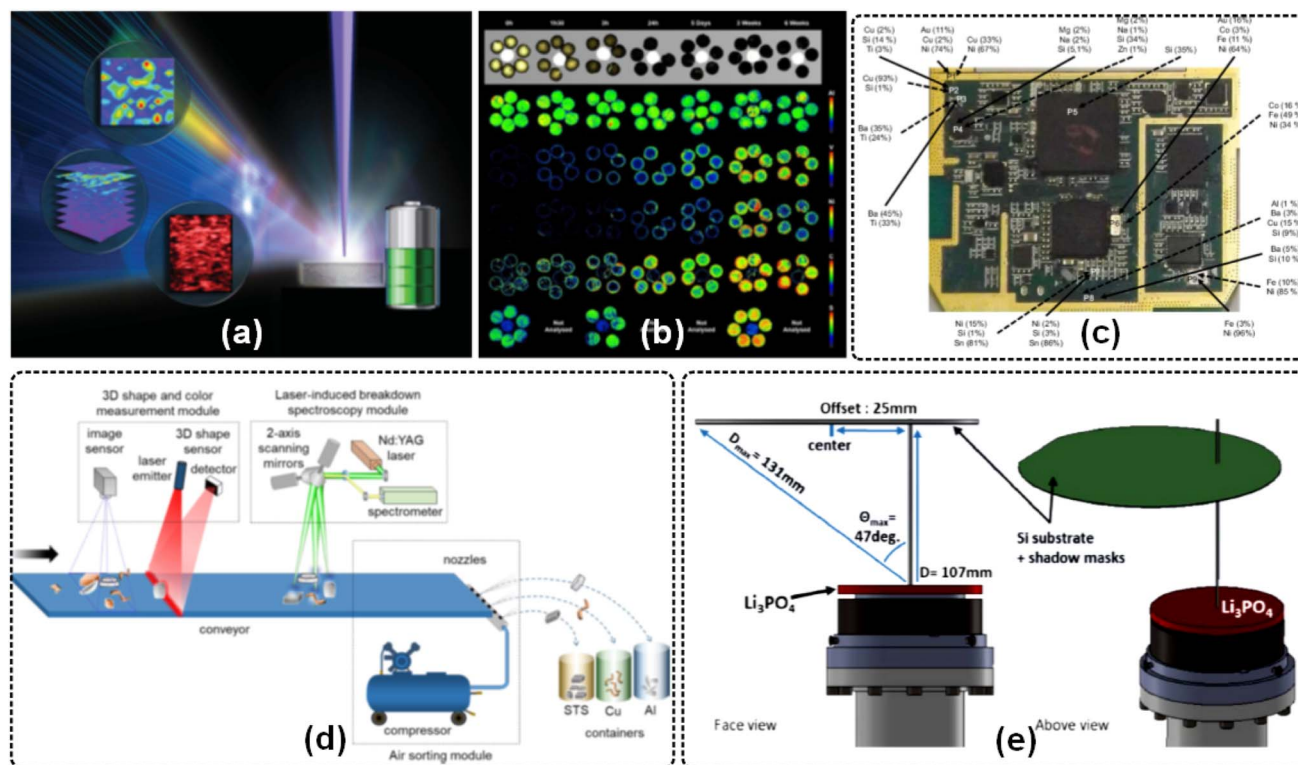
This journal is © The Royal Society of Chemistry 2025

J. Anal. At. Spectrom., 2025, 40, 665–678 | 671

**Fig. 7** Mineral analysis by the LIBS imaging approach: (a) optical images of the gemstone and five LIBS elemental images of Fe, Si, Cu, P, and Al in a gray color scale,[30] (b) distribution images of elements generated from the classical signal integration method from LIBS and PIL spectra,[76] (c) principle of elemental LIBS, molecular LIBS, and PIL experiments,[82] (d) the mean spectrum of the LIBS data set, the global intensity image, and elemental images generated with the conventional approach,[77] (e) elemental images (B, Ca, S, Mo, Fe, and Zn) of the mine core surface in the region represented by the rectangle,[79] (f) elemental and luminescence imaging of Kovdor fluorapatite.[82]

can well reflect the composition of the material.[128] Another approach is called calibration-free LIBS (CF-LIBS), which is a physical process that studies laser-induced plasma. According to the corresponding theories and practical assumptions, quantitative analysis can be conducted using experimental data measured by experiments and physical theoretical formulae.[129,130] But it is a consensus that developing a universal LIBS quantitative method is almost impossible. A more feasible approach is to develop specialized LIBS quantitative methods in specific fields to meet their application needs. Besides, how to

**672** | *J. Anal. At. Spectrom.*, 2025, **40**, 665–678

This journal is © The Royal Society of Chemistry 2025

Fig. 8  Industry and materials analysis by the LIBS imaging approach: (a) three-dimensional elemental imaging of Li-ion solid-state electrolytes using fs-LIBS,[102] (b) optical images of supports impregnated with asphaltenes and the corresponding LIBS images of the asphaltenes,[104](c) semi-quantitative information obtained using SEM-EDS for the surface (solid arrows) and crater (dotted arrows),[106](d) laboratory-scale automatic sorting system based on laser-induced breakdown spectroscopy,[97] and (e) relative positions of the target ($Li_3PO_4$; red) and substrate (Si wafer; green) during magnetron sputtering.[107]

improve the accuracy, precision, and sensitivity of LIBS quantitative imaging is also a key issue to be addressed in the future.

## 5.2  Technology upgrade proposal

**5.2.1  LIBS signal optimization.** The existence of signal uncertainty remains the biggest obstacle to qualitative and quantitative chemical analysis of LIBS, with original signal optimization being a key and difficult problem that needs to be overcome in the past, present, and future. The object of LIBS analysis is the dynamic plasma plume, in which the signal source varies dramatically with the short-time spatiotemporal evolution of the plasma expansion process.[131,132] Besides, in the process of LIBS measurement, signal uncertainty and measurement accuracy are also influenced by factors such as the matrix effect, self-absorption effect, and spectral overlap interference.[32] In order to solve the uncertainty problem of LIBS original signals, researchers mainly focus on two aspects: experimental methods and data processing and modeling methods. A universal truth is that the quality and integrity of the original signal have an important impact on the accuracy and reliability of model results. Therefore, it is necessary to use some experimental methods to improve the stability and reliability of LIBS imaging signals. Specifically, the double-pulse system,[133–135] spark discharge pulse re-excitation system,[136,137] microwave supplementary system,[138,139] resonance excitation

system,[140] flame supplementary system,[141] cavity confinement system,[142,143] magnetic field confinement system,[144,145] nano-particle and micro-nanostructure systems,[146] external gas and pressure systems,[147] light-field modulation system,[148,149] and ultrafast laser beam system[150] have been proposed. A summary of LIBS signal optimization methods is shown in Fig. 9.

**5.2.2  LIBS imaging resolution improvement**

*5.2.2.1 Spectral resolution.* On the basis of LIBS signal optimization, from the perspective of software and algorithms, image super-resolution reconstruction (ISRR) technology may become an effective way to solve the problem of lower spectral resolution.[151,152] ISRR technology refers to the restoration of a given low-resolution image to a corresponding high-resolution image by using a specific algorithm. The traditional super-resolution reconstruction algorithm mainly relies on basic digital image processing technology for reconstruction, which generally includes (1) interpolation-based super-resolution reconstruction, (2) degenerate model-based super-resolution reconstruction, and (3) learning-based super-resolution reconstruction. Besides, deep learning has begun to be widely applied in various fields, especially in the fields of image and vision, and convolutional neural networks have made great achievements, which has led more and more researchers to attempt to introduce deep learning into the field of super-resolution reconstruction.[153,154]
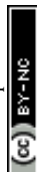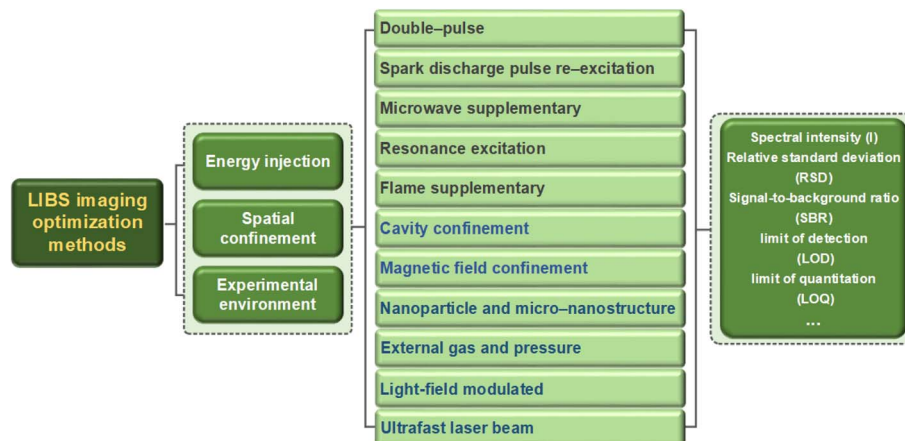
**Fig. 9**  A summary of LIBS optimization methods.

*5.2.2.2  Spatial resolution.* High-resolution LIBS images typically have greater pixel density, richer texture details, and higher reliability than low-resolution images. The most direct way to improve spatial resolution is to increase the point-to-point density of laser ablation, which puts forward higher requirements for beam quality and spot diameter. However, the LIBS system faces great challenges in providing the minimum spot size while maintaining overall beam parameter stability. Several solutions have been proposed at present: changing the laser wavelength (the limit value of the focused spot is proportional to the wavelength), changing the focal length of the objective lens (the focused spot is proportional to the focal length), and changing the diameter of the entrance pupil spot (the entrance pupil spot diameter is inversely proportional to the focal length); that is, using a short wavelength laser, a small focal length objective lens, a beam expander, or a spatial filter might be able to resolve the existing spatial resolution problem.

*5.2.2.3  Spectral sensitivity.* Existing LIBS imaging operations have high requirements for the flatness of samples. For some samples with uneven surfaces, the commonly used methods currently have low spectral sensitivity. A promising solution is to elongate the spatial distance of the focused beam, using

optical field modulation, self-focusing lens, femtosecond laser filamentation, and so on. This can further improve the spectral sensitivity and accuracy of LIBS imaging.

**5.2.3  Multiple technology integration.** Spectral analysis technology is the latest high-tech analytical tool in the field of analytical chemistry, which is receiving increasing attention from domestic and foreign analytical experts. At present, spectrum technology and spectrum instruments are based on optical principles, with precision machinery as the framework and electronic signal processing as the display.[32,155] Digitalization, intellectualization, and networking have become the new development directions of spectrum instruments, and multispectral data fusion may also become another "breakthrough point" in the development of spectral technology.

Modern spectral technology allows rapid, micro/non-destructive analysis of targets directly. Different types of spectrum measuring methods have different analysis focuses. In order to achieve a more comprehensive and accurate analysis, it is necessary to combine various analysis methods. The combination method optimizes and integrates different types of spectra to realize the complementary advantages of a single spectrum so as to obtain more comprehensive, reliable, and abundant
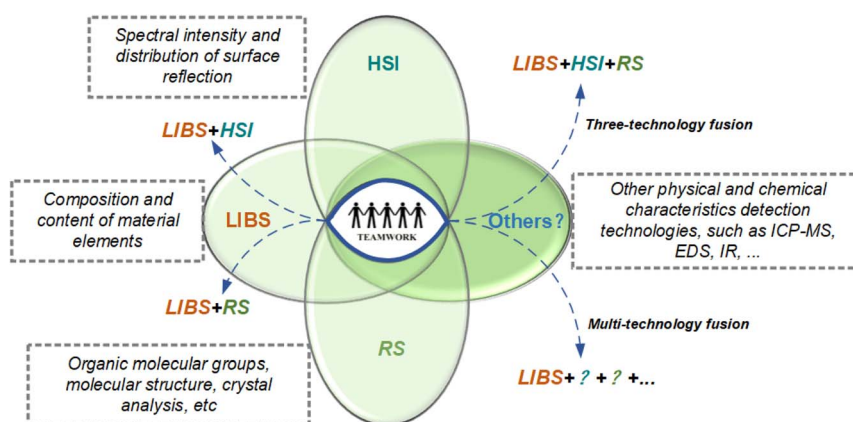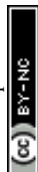


**Fig. 10**  Schematic diagram of multiple technology integration operations.

characteristic data, achieving the purpose of improving the accuracy and stability of model prediction.[31] The schematic diagram of multiple technology integration is shown in Fig. 10. There are currently mature technology integration cases, such as LIBS + HSI,[156] LIBS + RS,[157] LIBS + ICP-MS,[158] and so on. The joint usage of two or more technologies is the trend of future development and has important application value.

There are two ways to achieve the multi-technology integration. One depends on the degree of matching between hardware devices, such as HSI, RS, IR, *etc.*, and these technologies have the characteristics of being fast, *in situ*, and simple. Therefore, the combination of these technologies can improve the performance of LIBS spectral imaging technology without losing their respective advantages. Another way is low hardware compatibility, such as ICP-MS and EDS. First, image segmentation, ROI recognition, and feature classification are performed based on LIBS data. A more accurate component analysis of small sample ROIs is then performed using mass spectrometry or other techniques. Besides, LIBS-ICP-MS can provide full spectral and elemental information. Finally, a component content distribution map is drawn on the basis of feature correlation analysis.

## 6. Conclusion

LIBS has received more and more attention in the field of elemental imaging, mainly due to its advantages of rapid, *in situ*, small-invasive, and simultaneous detection of multi-elements, simple operation, and safety compared to other techniques. This review introduced the fundamental principle, operation, and data-processing methods of LIBS imaging and compared and discussed the types of LIBS 2D/3D imaging and micro-LIBS imaging. On this basis, the relevant applications in the fields of biomedicine, minerals, industry, materials, *etc.*, were introduced. Finally, four technological upgrade proposals, including LIBS signal optimization, spatial resolution improvement, multiple technology integration, and quantitative analysis, were proposed and discussed. All these will be further studied and overcome in the future, and LIBS imaging technology will be applied in more fields.

## Data availability

The data that support the findings of this study are available from the corresponding author or some open source website, upon reasonable request.

## Author contributions

Shangyong Zhao: investigation, conceptualization, writing – original draft & review, supervision, funding acquisition. Yuchen Zhao: writing – original draft & review & editing, validation. Yujia Dai: investigation. Ziyuan Liu: investigation. Zongyu Hou: investigation. Xun Gao: investigation, writing – original draft. Zhe Wang: writing – original draft, supervision, project administration, funding acquisition.

## Conflicts of interest

The authors declare that they have no known competing financial interests or personal relationships that could have appeared to influence the work reported in this paper.

## Acknowledgements

## References
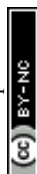
1 D. Wu, Y. Hu, H. Cheng and X. Ye, *Molecules*, 2023, **28**, 3601.

2 X. Jia, S. Li, D. Han, R. Chen, Z. Yao, B. Ning, Z. Gao and Z. Fan, *Crit. Rev. Food Sci. Nutr.*, 2021, **62**, 4706–4725.

3 Y. Qiu, X. Zhou, X. Tang, Q. Hao and M. Chen, *Materials*, 2023, **16**, 2253.

4 M. Yang, R. Bi, J. Wang, R. Yu and D. Wang, *Int. J. Miner., Metall. Mater.*, 2022, **29**, 965–989.

5 N. Balke, S. Kalnaus, N. J. Dudney, C. Daniel, S. Jesse and S. V. Kalinin, *Nano Lett.*, 2012, **12**, 3399–3403.

6 Z. Deng, X. Lin, Z. Huang, J. Meng, Y. Zhang, G. Ma, Y. Zhou, Y. Shen, H. Ding and Y. Huang, *Adv. Energy Mater.*, 2021, **11**, 2000806.

7 A. Limbeck, L. Brunnbauer, H. Lohninger, P. Porízka, P. Modlitbov, J. Kaiser, P. Janovszky, A. Keri and G. Galbacs, *Anal. Chim. Acta*, 2021, **1147**, 72e98.

8 B. Busser, S. Moncayo, J. Coll, L. Sancey and V. Motto-Ros, *Coord. Chem. Rev.*, 2018, **358**, 70–79.

9 G. L. P. A. Ramos, L. M. R. Esper and A. G. M. Gonzalez, *Int. J. Food Sci. Technol.*, 2024, **59**, 1187–1196.

10 I. Kim, C. Park, D. Shin and I. Yun, *IEEE Sens. J.*, 2021, **21**, 2256–2262.

11 Q. Wu, D. Xiao, N. Wang, F. Masis, W. Langbin and B. Li, *Talanta*, 2024, **266**, 125067.

12 R. Fritzsch, S. Hume, L. Minnes, M. J. J. Baker, G. A. A. Burley and N. T. T. Hunt, *Analyst*, 2020, **145**, 2014–2024.

13 J. Orsilli and S. Caglio, *Minerals*, 2024, **14**, 192.

14 S. S. Harilal, A. K. Shaik, E. J. Kautz, A. Devaraj, A. M. Casella and D. J. Senor, *J. Anal. At. Spectrom.*, 2024, **39**, 699–703.

15 J. D. Winefordner, I. B. Gornushkin, T. Correll, E. Gibb, B. W. Smith and N. Omenetto, *J. Anal. At. Spectrom.*, 2004, **19**, 1061e1083.

16 D. S. Francischini and M. A. Z. Arruda, *Microchem. J.*, 2021, **169**, 106526.

17 J. Caceres, F. Pelascini, V. Motto-Ros, S. Moncayo, F. Trichard, G. Panczer, A. Marín-Roldán, J. Cruz, I. Coronado and J. Martín-Chivelet, *Sci. Rep.*, 2017, **7**, 5080.

18 C. J. M. Lawley, A. M. Somers and B. A. Kjarsgaard, *J. Geochem. Explor.*, 2021, **222**, 106694.

This journal is © The Royal Society of Chemistry 2025

*J. Anal. At. Spectrom.*, 2025, **40**, 665–678 | **675**

19 V. Gardette, V. Motto-Ros, C. Alvarez-Llamas, L. Sancey, L. Duponchel and B. Busser, *Anal. Chem.*, 2023, **95**, 49–69.

20 L. Jolivet, M. Leprince, S. Moncayo, L. Sorbier, C.-P. Lienemann and V. Motto-Ros, *Spectrochim. Acta, Part B*, 2019, **151**, 41–53.

21 S. Zhao, Y. Zhao, Y. Dai, Z. Liu, H. Zha and X. Gao, *Front. Phys.*, 2024, **19**, 62500.

22 S. Zhao, C. Song, X. Gao, K. Guo, Z. Hao and J. Lin, *Results Phys.*, 2020, **19**, 103601.

23 S. Zhao, W. Song, Z. Houa and Z. Wang, *J. Anal. At. Spectrom.*, 2021, **36**, 1704–1711.

24 S. Zhao, W. Song, Y. Zhao, Z. Hou and Z. Wang, *Microchem. J.*, 2022, **183**, 107986.

25 D. Zhang, Y. Chu, S. Ma, Z. Sheng, F. Chen, Z. Hu, S. Zhang, B. Wang and L. Guo, *Appl. Surf. Sci.*, 2020, **534**, 147601.

26 E. M. Garcell and C. Guo, *J. Appl. Phys.*, 2018, **123**, 213103.

27 S. M. Pimenov, E. V. Zavedeev, B. Jaeggi and B. Neuenschwander, *Materials*, 2023, **16**, 795.

28 M. E. Shaheen, J. E. Gagnon and B. J. Fryer, *Opt. Lasers Eng.*, 2019, **119**, 18–25.

29 M. E. Shaheen and J. E. Gagnon, *Laser Phys.*, 2016, **26**, 116102.

30 S. Moncayo, L. Duponchel, N. Mousavipak, G. Panczer, F. Trichard, B. Bousquet, F. Pelascini and V. Motto-Ros, *J. Anal. At. Spectrom.*, 2018, **33**, 210–220.

31 S. Zhao, Y. Zhao, Z. Hou and Z. Wang, *Appl. Surf. Sci.*, 2023, **629**, 157415.

32 Z. Wang, M. S. Afgan, W. L. Gu, Y. Z. Song, Y. Wang, Z. Y. Hou, W. R. Song and Z. Li, *TrAC, Trends Anal. Chem.*, 2021, **143**, 116385.

33 P. Yin, E. Yang, Y. Chen, Z. Peng, D. Li, Y. Duan and Q. Lin, *Chem. Commun.*, 2021, **57**, 7312–7315.

34 M. Markiewicz-Keszycka, X. Cama-Moncunill, M. P. Casado-Gavalda, Y. Dixit, R. Cama-Moncunill, P. J. Cullen and C. Sullivan, *Trends Food Sci. Technol.*, 2017, **65**, 80–93.

35 J. Schreiner, F. Goetz-Neunhoeffer, J. Neubauer, S. Volkmann, S. Bergold, R. Webler and D. Jansen, *Powder Diffr.*, 2019, **34**, 143–150.

36 P. Mishra, A. Biancolillo, J. M. Roger, F. Marini and D. N. Rutledge, *TrAC, Trends Anal. Chem.*, 2020, **132**, 116045.

37 S. Marukatat, *Artif. Intell. Rev.*, 2023, **56**, 5445–5477.

38 J. Oh and N. Kwak, *Signal Process.*, 2024, **219**, 109421.

39 M. Kimura, *IEEE Access*, 2021, **9**, 129619–129625.

40 Z. Liu, R. Zheng, Y. Tian, B. Wang, J. Guo and Y. Lu, *J. Anal. At. Spectrom.*, 2022, **37**, 1134–1140.

41 S. Zhao, M. S. Afgan, H. Zhu and X. Gao, *Optik*, 2022, **25**, 16844.

42 W. Song, Z. Hou, W. Gu, H. Wang, J. Cui, Z. Zhou, G. Yan, Q. Ye, Z. Li and Z. Wang, *Fuel*, 2021, **306**, 121667.

43 K. R. Kim, G. Kim, J. Y. Kim, K. Park and K. W. Kim, *J. Anal. At. Spectrom.*, 2014, **29**, 76–84.

44 M. Gragston, P. Hsu, N. Jiang, S. Roy and Z. Zhang, *Appl. Opt.*, 2021, **60**, C114–C120.

45 A. Marín Roldán, M. Pisarčík, M. Veis, M. Držík and P. Veis, *Spectrochim. Acta, Part B*, 2021, **177**, 10655.

46 Z. Feng, J. Zhang, X. Li, Q. Gao and B. Li, *J. Phys. D: Appl. Phys.*, 2022, **55**, 505206.

47 S. A. Kalam, N. L. Murthy, P. Mathi, N. Kommu, A. K. Singh and S. V. Rao, *J. Anal. At. Spectrom.*, 2017, **32**, 1535–1546.

48 M. Shi, J. Wu, D. Wu, X. Guo, Y. Qiu, Y. Zhou, J. Li, H. Sun, X. Li and A. Qiu, *Spectrochim. Acta, Part B*, 2023, **209**, 106797.

49 C. Fabre, K. Trebus, A. Tarantola, J. Cauzid, V. Motto-Ros and P. Voudouris, *Spectrochim. Acta, Part B*, 2022, **194**, 106470.

50 C. Alvarez-Llamas, A. Tercier, C. Ballouard, C. Fabre, S. Hermelin, J. Margueritat, L. Duponchel, C. Dujardin and V. Motto-Ros, *J. Anal. At. Spectrom.*, 2024, **39**, 1077–1086.

51 R. Glaus and D. W. Hahn, *Spectrochim. Acta, Part B*, 2014, **100**, 116–122.

52 M. Martin, D. Hamm, S. Martin, S. Allman, G. Bell and R. Martin, *Minerals*, 2019, **9**, 103.

53 A. Botto, B. Campanella, S. Legnaioli, M. Lezzerini, G. Lorenzetti, S. Pagnotta, F. Poggialini and V. Palleschi, *J. Anal. At. Spectrom.*, 2019, **34**, 81–103.

54 K. Zabłocka-Słowińska, S. Płaczkowska, A. Prescha, K. Pawelczyk, I. Porebska, M. Kosacka, L. Pawlik-Sobecka and H. Grajeta, *J. Trace Elem. Med. Biol.*, 2018, **45**, 78–84.

55 S. Liao, S. O. Omage, L. Börmel, S. Kluge, M. Schubert, M. Wallert and S. Lorkowski, *Antioxidants*, 2022, **11**, 1785.

56 S. LI, X. Jiang, Y. Luo, B. Zhou, M. Shi, F. Liu and A. Sha, *Chemosphere*, 2019, **234**, 579–588.

57 R. B. N. Renata, G. R. A. Arely, L. M. A. Gabriela and M. L. M. Esther, *Biol. Trace Elem. Res.*, 2023, **201**, 1596–1614.

58 V. Gardette, L. Sancey, M. Leprince, L. Gate, F. Cosnier, C. Seidel, S. Valentino, F. Pelascini, J. -L. Coll, M. Peoc'h, V. Scolan, F. Paysant, V. Bonneterre, C. Dujardin, B. Busser and V. Motto-Ros, *Small Sci.*, 2024, **4**, 2300307.

59 V. H. C. Ferreira, V. Gardette, B. Busser, L. Sancey, S. Ronsmans, V. Bonneterre, V. Motto-Ros and L. Duponchel, *Anal. Chem.*, 2024, **96**, 7038–7046.

60 L. Zou, B. Kassim, J. P. Smith, J. D. Ormes, Y. Liu, Q. Tu and X. Bu, *Analyst*, 2018, **143**, 5000–5007.

61 H. Wei, Z. Zhao, Q. Lin and Y. Duan, *Biol. Trace Elem. Res.*, 2021, **199**, 1686–1692.

62 Q. Lian, X. Li, B. Lu, C. Zhu, J. Li and J. Chen, *IEEE Access*, 2023, **11**, 141915–141925.

63 P. Yin, B. Hu, Q. Li, Y. Duan and Q. Lin, *IEEE Trans. Instrum. Meas.*, 2021, **70**, 4006207.

64 K. Kiss, A. Sindelaova, L. Krbal, V. Stejskal, K. Mrazova, J. Vrabel, M. Kaska, P. Modlitbová, P. Porízka and J. Kaiser, *J. Anal. At. Spectrom.*, 2021, **36**, 909–916.

65 S. Moncayo, F. Trichard, B. Busser, M. Sabatier-Vincent, F. Pelascini, N. Pinel, I. Templier, J. Charles, L. Sancey and V. Motto-Ros, *Spectrochim. Acta, Part B*, 2017, **133**, 40–44.

66 B. Busser, A. Bulin, V. Gardette, H. Elleaume, F. Pelascini, A. Bouron, V. Motto-Ros and L. Sancey, *J. Neurosci. Methods*, 2022, **379**, 109676.

67 M. Leprince, L. Sancey, J. L. Coll, V. Motto-Ros and B. Busser, *Med. Sci.*, 2019, **35**, 682–688.

68 Y. Gimenez, B. Busser, F. Trichard, A. Kulesza, J. M. Laurent, V. Zaun, F. Lux, J. M. Benoit, G. Panczer,

**676** | *J. Anal. At. Spectrom.*, 2025, **40**, 665–678

This journal is © The Royal Society of Chemistry 2025

P. Dugourd, O. Tillement, F. Pelascini, L. Sancey and V. Motto-Ros, *Sci. Rep.*, 2016, **6**, 29936.

69 B. Busser, S. Moncayo, F. Trichard, V. Bonneterre, N. Pinel, F. Pelascini, P. Dugourd, J. L. Coll, M. D'Incan, J. Charles, V. Motto-Ros and L. Sancey, *Mod. Pathol.*, 2018, **31**, 378–384.

70 J. Choi, S. Shin, Y. Moon, J. Han, E. Hwang and S. Jeong, *Spectrochim. Acta, Part B*, 2021, **179**, 106090.

71 J. P. Smith, L. Zou, Y. Liu and X. Bu, *Spectrochim. Acta, Part B*, 2020, **165**, 105769.

72 Q. Lin, S. Wang, Y. Duan and V. V. Tuchin, *J. Biophotonics*, 2021, **14**, e202000479.

73 A. Buzatu, G. Damian, N. Buzgar, P. Andras, A. L. Apopeia, A. E. Maftei and S. Milovska, *Vib. Spectrosc.*, 2017, **89**, 49–56.

74 J. A. Meima and D. Rammlmair, *Chem. Geol.*, 2020, **532**, 119376.

75 C. Fabre, D. Devismes, S. Moncayo, F. Pelascini, F. Trichard, A. Lecomte, B. Bousquet, J. Cauzid and V. Motto-Ros, *J. Anal. At. Spectrom.*, 2018, **33**, 1345–1353.

76 A. Nardecchia, A. de Juan, V. Motto-Ros, M. Gaft and L. Duponchel, *Anal. Chim. Acta*, 2022, **1192**, 339368.

77 A. Nardecchia, C. Fabre, J. Cauzid, F. Pelascini, V. Motto-Ros and L. C. Duponchel, *Anal. Chim. Acta*, 2020, **1114**, 66–73.

78 T. Chen, L. Sun, H. Yu, W. Wang, L. Qi, P. Zhang and P. Zeng, *Appl. Geochem.*, 2022, **136**, 105135.

79 F. Trichard, S. Moncayo, D. Devismes, F. Pelascini, J. Maurelli, A. Feugier, C. Sasseville, F. Surmad and V. Motto-Ros, *J. Anal. At. Spectrom.*, 2017, **32**, 1527–1534.

80 W. Huang, C. He, Y. Wang, W. Zhao and L. Qiu, *J. Anal. At. Spectrom.*, 2020, **35**, 2530–2535.

81 K. Rifai, L. Ç. Özcan, F. R. Doucet, K. Rhoderick and F. Vidal, *Minerals*, 2020, **10**, 207.

82 M. Gaft, Y. Raichlin, F. Pelascini, G. Panzer and V. Motto Ros, *Spectrochim. Acta, Part B*, 2019, **151**, 12–19.

83 J. Klus, P. Mikysek, D. Prochazka, P. Pořízka, P. Prochazkova, J. Novotny, T. Trojek, K. Novotny, M. Slobodník and J. Kaiser, *Spectrochim. Acta, Part B*, 2016, **123**, 143–149.

84 O. Syta, B. Wagner, E. Bulska, D. Zielińska, G. Z. Zukowska, J. Gonzalez and R. Russo, *Talanta*, 2108, **179**, 784–791.

85 I. Krempl, K. Novotný, V. Wertich, R. Skoda, V. Kanický and J. Leichmann, *Spectrochim. Acta, Part B*, 2023, **206**, 106734.

86 J. Aramendia, L. Gómez-Nubla, S. F. O. de Vallejuelo, K. Castro, G. Arana and J. M. Madariaga, *J. Raman Spectrosc.*, 2019, **50**, 193–201.

87 M. A. Speranc, F. W. B. de Aquino, M. A. Fernandes, A. Lopez-Castillo, R. L. Carneiro and E. R. Pereira-Filho, *Geostand. Geoanal. Res.*, 2017, **41**, 273–282.

88 C. Sandoval-Munoz, G. Velasquez, J. Alvarez, F. Perez, M. Velasquez, S. Torres, D. Sbarbaro-Hofer, V. Motto-Ros and J. Yanez, *J. Anal. At. Spectrom.*, 2022, **37**, 1981–1993.

89 W. Nikonow, D. Rammlmair, J. A. Meima and M. C. Schodlok, *Mineral. Petrol.*, 2019, **113**, 417–431.

90 C. Fabre, K. Trebus, A. Tarantola, J. Cauzid, V. Motto-Ros and P. Voudouris, *Spectrochim. Acta, Part B*, 2022, **194**, 106470.

91 J. R. Chirinos, D. D. Oropeza, J. J. Gonzalez, H. Hou, M. Morey, V. Zorba and R. E. Russo, *J. Anal. At. Spectrom.*, 2014, **29**, 1292–1298.

92 T. Lopes, D. Capela, M. F. S. Ferreira, D. Guimarães, P. A. S. Jorge and N. A. Silva, *Appl. Spectrosc.*, 2024, **78**, 753–759.

93 J. A. Meima and D. Rammlmair, *Chem. Geol.*, 2020, **532**, 119376.

94 C. Schiavo, L. Menichetti, E. Grifoni, S. Legnaioli, G. Lorenzetti and F. Poggialini, *J. Instrum.*, 2016, **11**, C080002.

95 G. S. Senesi, B. Campanella, E. Grifoni, S. Legnaioli, G. Lorenzetti, S. Pagnotta, F. Poggialini, V. Palleschi and O. D. Pascale, *Spectrochim. Acta, Part B*, 2018, **143**, 91–97.

96 X. Wang, G. Zhang, A. Li, Y. Wang, H. Cui, W. Zhao and L. Qiu, *Spectrochim. Acta, Part B*, 2023, **207**, 106759.

97 A. Cugerone, B. Cenki-Tok, E. Oliot, M. Muñoz, F. Barou, V. Motto-Ros and E. Le Goff, *Geology*, 2020, **48**, 236–241.

98 D. Fougerouse, A. Cugerone, S. M. Reddy, K. Luo and V. Motto-Ros, *Geochim. Cosmochim. Acta*, 2023, **346**, 223–230.

99 S. Park, J. Lee, E. Kwon, D. Kim, S. Shin, S. Jeong and K. Park, *Int. J. Precis. Eng. Manuf. – Green Technol.*, 2022, **9**, 695–707.

100 M. Weiss, Z. Gajarska, H. Lohninger, M. Marchetti-Deschmann, G. Ramer, B. Lendl and A. Limbeck, *Anal. Chim. Acta*, 2022, **1195**, 339422.

101 W. Song, Y. Fu, S. Zhao, Y. Zhao, H. Wang and Z. Wang, *Constr. Build. Mater.*, 2023, **392**, 131834.

102 H. Hou, L. Cheng, T. Richardson, G. Chen, M. Doeff, R. Zheng, R. Russo and V. Zorba, *J. Anal. At. Spectrom.*, 2015, **30**, 2295–2302.

103 F. Trichard, F. Gaulier, J. Barbier, D. Espinat, B. Guichard, C. P. Lienemann, L. Sorbier, P. Levitz and V. Motto-Ros, *J. Catal.*, 2018, **363**, 183–190.

104 L. Jolivet, L. Catita, O. Delpoux, C. P. Lienemann, L. Sorbier and V. Motto-Ros, *J. Catal.*, 2021, **401**, 183–187.

105 D. V. Babos, J. F. K. Ramos, G. C. Francisco, V. D. M. Benites and D. M. B. P. Milori, *J. Opt. Soc. Am. B*, 2023, **40**, 654–660.

106 R. R. V. Carvalho, J. A. O. Coelho, J. M. Santos, F. W. B. Aquino, R. L. Carneiro and E. R. Pereira-Filho, *Talanta*, 2015, **134**, 278–283.

107 W. Berthou, M. Legallais, B. Bousquet, V. Motto-Ros and F. L. Cras, *Spectrochim. Acta, Part B*, 2024, **215**, 106906.

108 C. M. Ahamer, K. M. Riepl, N. Huber and J. D. Pedarnig, *Spectrochim. Acta, Part B*, 2017, **136**, 56–65.

109 J. Fernandes, L. Sorbier, S. Hermelin, J.-M. Benoit, C. Dujardin, C.-P. Lienemann, J. Bernard and V. Motto-Ros, *Spectrochim. Acta, Part B*, 2024, **221**, 107047.

110 W. Berthou, M. Legallais, S. Sorieul, G. Yildirim, B. Bousquet, V. Motto-Ros and F. Le Cras, *Adv. Energy Mater.*, 2024, **14**, 2400656.

111 B. le Bellego, V. Motto-Ros, B. Luais, C. Fabre, C. Dalou, P. Condamine and L. Tissandier, *Spectrochim. Acta, Part B*, 2024, **222**, 107059.

112 D. Zhang, Y. Chu, S. Ma, Z. Sheng, F. Chen, Z. Hu, S. Zhang, B. Wang and L. Guo, *Appl. Surf. Sci.*, 2020, **534**, 147601.

This journal is © The Royal Society of Chemistry 2025

*J. Anal. At. Spectrom.*, 2025, **40**, 665–678 | **677**

113 Y. Meng, C. Gao, Z. Lin, W. Hang and B. Huang, *Nanoscale Adv.*, 2020, **2**, 3983–3990.

114 F. Trichard, L. Sorbier, S. Moncayo, Y. Blouët, C. P. Lienemann and V. Motto-Ros, *Spectrochim. Acta, Part B*, 2017, **133**, 45–51.

115 L. Brunnbauer, M. Jirku, C. D. Quarles Jr and A. Limbeck, *Talanta*, 2024, **269**, 125500.

116 J. O. Caceres, F. Pelascini, V. Motto-Ros, S. Moncayo, F. Trichard, G. Panczer, A. Marín-Roldán, J. A. Cruz, I. Coronado and J. Martín-Chivelet, *Sci. Rep.*, 2017, **7**, 5080.

117 N. Hausmann, P. Siozos, A. Lemonis, A. C. Colonese, H. K. Robson and D. Anglos, *J. Anal. At. Spectrom.*, 2017, **32**, 1467–1472.

118 L. Krajcarova, K. Novotny, M. Kummerova, J. Dubova, V. Gloser and J. Kaiser, *Talanta*, 2017, **173**, 28–35.

119 C. Zhao, D. Dong, X. Du and W. Zheng, *Sensors*, 2016, **16**, 1764.

120 R. R. Gamela, M. A. Speranca, D. F. Andrade and E. R. Pereira-Filho, *Anal. Methods*, 2019, **11**, 5543–5552.

121 Q. Tang, M. Zhong, P. Yin, Z. Zhang, Z. Chen, G. Wu and Q. Lin, *Spectrosc. Spectr. Anal.*, 2023, **43**, 1485–1488.

122 Y. Dixit, M. P. Casado-Gavalda, R. Cama-Moncunill, X. Cama-Moncunill, M. Markiewicz-Keszycka, F. Jacoby, P. J. Cullen and C. Sullivan, *J. Food Eng.*, 2018, **216**, 120–124.

123 M. Lopez-Lopez, C. Alvarez-Llamas, J. Pisonero, C. Garcıa-Ruiz and N. Bordel, *Forensic Sci. Int.*, 2017, **273**, 124–131.

124 N. Herreyre, A. Cormier, S. Hermelin, C. Oberlin, A. Schmitt, V. Thirion-Merle, A. Borlenghi, D. Prigent, C. Coquide, A. Valois, C. Dujardin, P. Dugourd, L. Duponchel, C. Comby-Zerbino and V. Motto-Ros, *J. Anal. At. Spectrom.*, 2023, **38**, 730–741.

125 Y. Zhang, X. Ren, Z. Chen, W. Chen, Z. Zhang, X. Liu, W. Xu, J. Liu and C. Li, *Remote Sens.*, 2023, **15**, 1494.

126 L. Guo, Z. Hao, M. Shen, W. Xiong, X. He, Z. Xie, M. Gao, X. Li, X. Zeng and F. Lu, *Opt. Express*, 2013, **21**, 18188–18195.

127 J. Yu, Z. Hou, Y. Ma, T. Li, Y. Fu, Y. Wang, Z. Li and Z. Wang, *Spectrochim. Acta Part B At. Spectrosc.*, 2020, **174**, 105992.

128 W. Song, Z. Song, J. Vincent, H. Wang and Z. Wang, *Talanta*, 2020, **216**, 120920.

129 T. A. Alrebdi, A. Fayyaz, H. Asghar, A. Zaman, M. Asghar, F. H. Alkallas, A. Hussain, J. Iqbal and W. Khan, *Molecules*, 2022, **27**, 3754.

130 Z. Lu, D. Zhang, W. Wang, F. Chen, Y. Xu, J. Nie, Y. Chu and L. Guo, *TrAC, Trends Anal. Chem.*, 2022, **152**, 116618.

131 Y. Fu, Z. Hou, T. Li, Z. Li and Z. Wang, *Spectrochim. Acta, Part B*, 2019, **155**, 67–78.

132 Y. Fu, W. Gu, Z. Hou, S. A. Muhammed, T. Li, Y. Wang and Z. Wang, *Front. Phys.*, 2021, **16**, 22502.

133 S. Zhao, C. Song, X. Gao and J. Lin, *Results Phys.*, 2019, **15**, 102736.

134 J. Shao, Y. Zhang and A. Chen, *Photonics*, 2023, **10**, 783.

135 C. P. D. Morais, D. V. Babos, V. C. Costa, J. B. Neris, G. Nicolodelli, M. C. Mitsuyuki, F. F. Mauad, S. Mounier and D. M. B. P. Milori, *Sci. Total Environ.*, 2022, **837**, 155699.

136 Q. Wang, A. Chen and X. Gao, *J. Anal. At. Spectrom.*, 2024, **39**, 261–268.

137 Y. Wang, X. He and C. Wang, *J. Anal. At. Spectrom.*, 2023, **38**, 1643–1651.

138 S. J. Chen, A. Iqbal, M. Wall, C. Fumeauxa and Z. T. Alwahabi, *J. Anal. At. Spectrom.*, 2017, **32**, 1508–1518.

139 Y. Ikeda, J. Ampadu Ofosu and I. Wakaida, *Spectrochim. Acta, Part B*, 2020, **171**, 105933.

140 S. Ma, Y. Liu, H. Tian, L. Guo and D. Dong, *J. Anal. At. Spectrom.*, 2023, **38**, 342–346.

141 Y. Song, W. Song, L. Li, W. Gu, K. Kou, M. S. Afgan, Z. Hou, Z. Li and Z. Wang, *Opt. Lasers Eng.*, 2023, **162**, 107433.

142 S. Zhao, X. Gao, A. Chen and J. Lin, *Appl. Phys.*, 2020, **126**, 7.

143 Z. Wang, Z. Hou, S. Lui, D. Jiang, J. Liu and Z. Li, *Opt. Express*, 2012, **20**, A1011–A1018.

144 M. A. Khan, S. Bashir, N. A. Chishti, E. Bonyah, A. Dawood and Z. Ahmad, *AIP Adv.*, 2023, **13**, 015017.

145 S. Mushtaq, K. Siraj, M. S. A. Rahim, S. U. Q. Younas, W. Asad, N. Shahzad and A. Latif, *Appl. Spectrosc.*, 2023, **77**, 393–404.

146 Y. Wang, Y. Bu, Y. Cai and X. Wang, *J. Anal. At. Spectrom.*, 2023, **38**, 121–130.

147 J. Yu, Z. Hou, Y. Ma, T. Li, Y. Fu, Y. Wang, Z. Li and Z. Wang, *Spectrochim. Acta, Part B*, 2020, **174**, 105992.

148 S. Zhao, Y. Zhao, Z. Hou and Z. Wang, *Spectrochim. Acta, Part B*, 2023, **203**, 106666.

149 Z. Hou, M. S. Afgan, S. Sheta, J. Liu and Z. Wang, *J. Anal. At. Spectrom.*, 2020, **35**, 1671–1677.

150 S. Zhao, Y. Zhao, Y. Dai, Z. Liu and X. Gao, *Spectrochim. Acta, Part B*, 2024, **218**, 106982.

151 M. Yamanaka, N. I. Smith and K. Fujita, *Microscopy*, 2014, **63**, 177–192.

152 C. Zhou and A. Xiong, *Sensors*, 2023, **23**, 1923.

153 Y. Huang, W. Bian, B. Jie, Z. Zhu and W. Li, *Signal Image Video P*, 2024, **18**, 1619–2641.

154 X. Chen, Y. Wu, J. Chen, J. Wang and K. Zeng, *IET Signal Process.*, 2023, **17**, e12205.

155 Z. Wang, T. Yuan, Z. Hou, W. Zhou, J. Lu, H. Ding and X. Zeng, *Front. Phys.*, 2014, **9**, 419–438.

156 S. Zhao, Z. Hou and Z. Wang, *J. Anal. At. Spectrom.*, 2024, **39**, 306–309.

157 A. Nardecchia, A. D. Juan, V. Motto-Ros, C. Fabre and L. Duponchel, *Spectrochim. Acta Part B At. Spectrosc.*, 2022, **198**, 106571.

158 M. Hola, K. Novotny, J. Dobes, I. Krempl, V. Wertich, J. Mozola, M. Kubes, V. Faltusova, J. Leichmann and V. Kanicky, *Spectrochim. Acta, Part B*, 2021, **186**, 106312.

678 | *J. Anal. At. Spectrom.*, 2025, **40**, 665–678

This journal is © The Royal Society of Chemistry 2025